Advances in Water Resources 194 (2024) 104851

Contents lists available at ScienceDirect

Advances in Water Resources

journal homepage: www.elsevier.com/locate/advwatres

Sub-daily precipitation returns levels in ungauged locations: Added value of combining observations with convection permitting simulations

Giuseppe Formetta [a,*], Eleonora Dallan [b], Marco Borga [b], Francesco Marra [c]

[a] Department of Civil, Environmental and Mechanical Engineering, University of Trento, Trento, Italy
[b] Department of Land Environment Agriculture and Forestry, University of Padova, Legnaro, Italy
[c] Department of Geosciences, University of Padova, Padova, Italy

ARTICLE INFO

Keywords:
Extreme rainfall
Convective permitting climate models
Rainfall return levels in ungauged locations

ABSTRACT

Extreme rainfall events trigger natural hazards, including floods and debris flows, posing serious threats to society and the economy. Accurately quantifying extreme rainfall return levels in ungauged locations is crucial for improving flood protection infrastructure and mitigating water-related risks. This paper quantifies the added value of combining rainfall observations with Convection Permitting Model (CPM) simulations to estimate sub-daily extreme rainfall return levels in ungauged locations. We assess the performance of CPM-informed estimates of extreme return level against a traditional interpolation techniques. We find that kriging methods with external drift outperform inverse distance weighting for both traditional and CPM-informed approaches. We then assess the effectiveness of the two methods under different scenarios of station density. At the highest station density (1/196 km^2), traditional interpolation methods outperform the CPM-informed method for durations under 6 h. The performance becomes comparable between 6 and 24 h. For lower station densities (1/400 and 1/800 km^2), the CPM-informed method outperforms the traditional method, with average reductions in fractional standard error of 24 %, 13 %, and 8 % for return periods of 2, 10 and 50 years, respectively for a rain gauge density of 1/800 km^2, and 16 %, 8 %, and 3 % for density of 1/400 km^2. Information from CPM simulations can thus be useful for estimating sub-daily extreme rainfall events in ungauged sites, particularly in data-scarce areas in which the density of rain gauges is low.

1. Introduction

Extreme sub-daily precipitation can lead to natural hazards, such as flash-floods, urban floods and debris flows. Worldwide, the number of reported damaging events for flash and general floods is growing, and their economic damages are strongly increasing, with a trend of 0.1 (for flash floods) and 0.7 billion (for general floods) US$2016/year over the last 40 years (e.g. Formetta and Feyen 2019). Accurate estimates of sub-daily return levels are crucial not only for reliable planning and designing of water-related infrastructure (i.e. quantifying the so-called design event) but also for advancing the quantification of disaster risks, and mitigating losses and damages (e.g. UNSIDR 2015).

Typically, the at-site rainfall frequency analysis consists in locally identifying the parameters of an extreme-value distribution and using them to compute the return levels relevant for the location of interest. The prediction of return levels in ungauged locations, i.e. locations where rainfall is not directly measured, is stated among the main objectives in several calls raised by different scientific communities since long time (e.g. Sivapalan et al. 2003), and still remains among the unsolved problems in hydrology (e.g. Blöschl et al. 2019). Regionalization techniques have been developed to reduce the parameter estimation uncertainty at gauged locations and to estimate the design rainfall in ungauged sites (see Claps et al. 2022 for a comprehensive review). Examples of the most applied techniques involve: (i) pooling together scaled rain-gauges measurements that belong to a homogenous region in order to estimate in a more robust way the parameters of the common (i.e. regional) underlying extreme value distribution (e.g. Hosking and Wallis 1997; Institute of Hydrology, 1999); (ii) using spatial interpolating algorithms to extend the (previously estimated) at-site rainfall return levels to ungauged locations (e.g. Szolgay et al. 2009); (iii) using spatial interpolating algorithms to extend the (previously estimated) at-site parameters of the extreme value distribution to ungauged locations, and use them to estimate the rainfall return levels (e.g. Ceresetti et al. 2012, Yin et al. 2018, Schellander et al. 2019).

* Corresponding author.
E-mail address: giuseppe.formetta@unitn.it (G. Formetta).

https://doi.org/10.1016/j.advwatres.2024.104851
Received 25 June 2024; Received in revised form 17 September 2024; Accepted 3 November 2024
Available online 4 November 2024

Interpolation methods are traditionally classified in two families: deterministic and geostatistical. The former uses deterministic mathematical functions to predict values of interest in ungauged sites, such as spatial distances for the Nearest Neighbour (e.g. Thiessen 1911, Tabios III and Salas 1985), Inverse Distance Weighted (e.g. Shepard 1968) methods, or the degree of smoothing for radial basis function (e.g. Hosseini et al. 2016, Adhikary and Dash 2017). The latter accounts for statistical properties (i.e., spatial autocorrelation) among sample points, uses the variogram to quantify the spatial variability of analysed phenomena (e.g. Goovaerts 1997), and provides unbiased estimates with minimum variance at ungauged locations (e.g. ordinary kriging, OK). Several studies demonstrated that geostatistical algorithms outperform deterministic methods for spatial interpolation of rainfall fields (e.g. Pellicone et al. 2018, Berndt and Haberlandt 2018), and that including the effects of secondary information (i.e. covariates such as elevation) in multivariate kriging procedures is beneficial for extreme rainfall interpolation (e.g. Faulkner and Prudhomme 1998, Zou et al. 2021).

Das et al. (2020) compared different approaches (i.e. interpolation of summary statistics of data represented by L-moments, interpolation of the Generalised extreme value distribution, and interpolation of the rainfall return levels) and different interpolation methods (IDW, OK, and KED) to estimate extreme rainfall in northeastern part of China. Results showed that interpolating the using the KED with mean annual precipitation as secondary variable provided the most accurate results in their study area.

Yet, the interpolation of sub-daily rainfall return levels remains challenging because the spatial variability of the underlying precipitation fields may be larger than the daily, and the number of available stations is lower than for the daily rainfall return levels. In fact, several studies pointed out that the sparseness of the currently available gauge networks is not adequate to capture and effectively reflect the variability of the precipitation fields (Kidd et al., 2017), especially for short duration extreme events (e.g. Lengfeld et al. 2020).

Regional climate models and numerical weather prediction offer a possibility to overcome these limitations by solving the atmospheric dynamic fundamental equations at fine scales (e.g. Sun et al. 2014, Brotzge et al. 2023, Giorgi 2019). Their modelled precipitation fields have been successfully assessed against measured data (e.g. Towler et al. 2020, Ozkaya 2023) or used in combination with learning methods, such as neural networks (e.g. Zhang et al. 2023). However, when compared against extreme measured precipitations they still show some shortcomings and biases (e.g. Knist et al. 2020, Poschlod 2021), attributed to orographic conditions and model limitations.

Recently, CPMs are increasingly gaining attention for simulating extreme rainfall fields, since they explicitly represent the deep convection (e.g. Ban et al. 2020, 2014, Kendon et al. 2012) using few-kilometres horizontal resolutions. This resolution is high enough ($\leq$ 4 km) to allow an explicit treatment of convection without the use of convection parameterization schemes (e.g. Kendon et al. 2017). However, CPMs have the limitation of being computationally expensive, therefore recent applications are generally available over relatively small domains and cover short temporal periods (e.g. Fosser et al. 2015, Berthou et al. 2020).

Only very recently, a few studies demonstrated the added value of CMPs simulations in rainfall statistical analysis over the baseline period. For example, Shmilovitz et al. (2023) combined sub-daily rainfall intensity information from raingauges and CPM weather model to understand the frequency of sediment mobilization along cliff and sub-cliff slopes in the Central Negev Desert.

In order to interpolate extreme precipitation of several durations in ungauged locations over Eastern Canada, Jalbert et al. (2022) used the long-term average daily precipitation from a (12 km 3-hourly resolution) regional climate model as covariate. They found that their proposed methodology generally improves the Environment and Climate Change Canada reference method, which has been used as comparison.

Poschlod and Koh (2024) combined statistics from daily resolution rainfall data from a high-resolution convection-permitting climate model (i.e. the Weather and Forecasting Research) and rain gauge observations to estimate high return levels of daily precipitation over Germany. They used a block (annual) maxima approach and built three spatial Generalized Extreme Value models using in turn (i) classical topographic information (i.e. latitude, longitude and elevation), and adding (ii) CPM mean annual rainfall first and, (iii) CPM based parameters of the distribution as covariates. Results show that the proposed models (ii) and (iii) have lower bias in the return level estimation with respect to the model (i), based on classical topographic information only.

In this paper we aim at quantifying the added value of the physics-based information provided by CPM simulations for the estimation of extreme precipitation return levels in ungauged locations. We extend over the pioneering work of Poschlod and Koh (2024) by extending our study to sub-daily (down to hourly) temporal scales. We reach this goal by: (1) combining for the first time at-site rain gauge measurements with CPM sub-daily rainfall simulations, and (2) testing the prediction of moderate to extreme rainfall return levels, from hourly to daily durations, in ungauged locations.

To exploit the strength of CPM sub-daily rainfall simulations and to compensate their limitation in record length, we use a non-asymptotic statistical framework which accounts for ordinary events (not only annual maxima). The newly proposed methodology is quantitively compared against traditional regionalization approaches for predicting sub-daily extreme rainfall in ungauged locations. We also quantified the influence of different interpolation techniques and varying densities of stations where observations are available through a controlled Monte Carlo experiment.

The paper is organized in other 5 Sections where we present the data used, the proposed regionalization framework, the results and their discussion, and finally we draw the main conclusions.

2. Study area and data

This study focuses on two Italian regions Trentino Alto-Adige and Veneto, located in northeast Italy (see Fig. 1). The area is around 32,000 km^2 in size and it is peculiar because it covers a great variety of climates and precipitation formation processes, including: (i) a mountainous and orographically complex region (north-western portion, e.g. Fliri 1975) which receive relatively low amounts of precipitation (about 900 mm/year) due to the shielding offered by the surrounding; (ii) a central pre-alpine part, where larger amounts are typically observed, up to 2300–2500 mm/year (e.g. Isotta et al. 2014); and, (iii) a flat area dominated by the contrast between the Adriatic Sea and coastal land (south-eastern portion).

The rainfall data used in this study are based on (i) gauge measurements, and (ii) simulated data from a convection-permitting model. The former dataset is based on quality-controlled, 5 min temporal resolution rainfall timeseries collected at 174 reheated rain gauges. We considered rain gauges with a record length from 14 to 37 complete years, i.e. years in which less than 10 % of the 5 min time intervals are flagged as missing or low quality (e.g. Marra et al. 2021a, Formetta et al. 2022, Dallan et al. 2023). The latter (i.e. the modelled CPM rainfall data) are provided by the ETH Zurich and are based on the COSMO-crCLIM, the climate version of the COSMO (Consortium for Small Scale Modelling) non-hydrostatic, limited-area climate model (Rockel et al., 2008).

The model domain covers the so called “greater Alpine region”, defined under the Flagship Pilot Study on Convective Phenomena over Europe and the Mediterranean (FPS-Convection; Coppola et al. 2020) which is part of the Coordinated Regional Climate Downscaling Experiment (CORDEX) program.

The simulation covers the period 2000–2009 (i.e. 10 years) at hourly scale and at 2 km spatial resolution, being nested in a 12 km European regional climate model driven by ERA Interim (Dee et al. 2011).

We aggregated the 5 min gauged rainfall data at a 1 h temporal

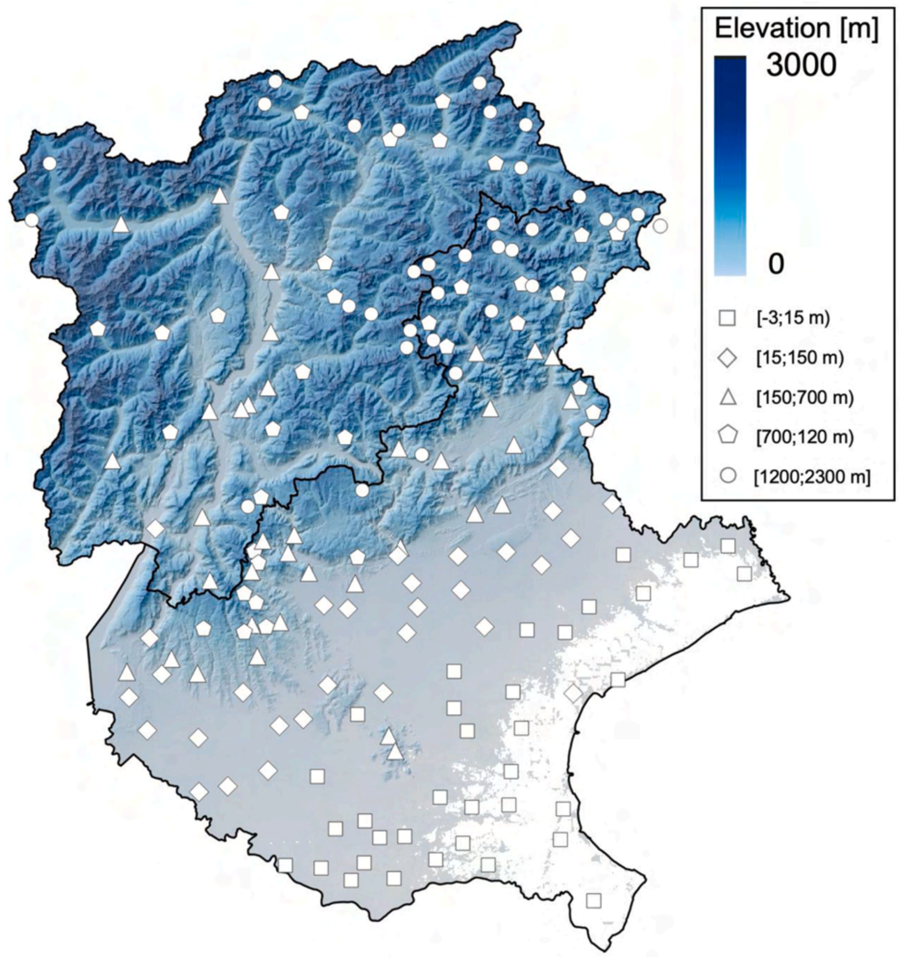

Fig. 1. Study area, digital elevation model and location of the rain gauges reported with different symbols by elevation classes (see the legend).

resolution to be consistent with the modelled CPM rainfall, obtaining the so called gauged based precipitation time series. Following the methodology proposed in Dallan et al. (2023) we extracted the CPM hourly precipitation data at the nearest CPM grid of each rain gauge, obtaining the "station-collocated" CPM precipitation time series.

FPS-Convection aims to improve the model representation of: (i) fine-scale surface heterogeneities/orography and (ii) surface fields variations which in turn are crucial for a more realistic modelling of deep convection processes and a more accurate simulation of mountain, coastal, and urbanized areas.

3. Methodology

3.1. Return level estimation

We estimate return levels using a non-asymptotic approach able to leverage information from more data than traditional extreme value methods. Specifically, we adopt the Simplified Metastatistical Extreme Value (SMEV) approach (Marra et al., 2019; 2020). This method estimates the non-exceedance probability $G(x)$of an extreme precipitation intensity $x[mmh^{-1}]$ based on the ordinary events, that are the independent samples of the analysed stochastic process (Marani and Ignaccolo, 2015):

$$G(x) \approx F(x;\theta)^n \tag{1}$$

where $F(x;\theta)$ is the cumulative distribution function describing the right tail of the ordinary events, θ its parameters, and n [-] the average yearly number of ordinary events. The SMEV is a simplified formulation of the Metastatistical Extreme Value distribution (Marani and Ignoccolo, 2015) in which inter-annual variability is neglected. In this approximation, all ordinary events are used for the estimation of θ. This allows to focus on the right tail of $F(x;\theta)$ which is the one related to extremes and yields a more robust parameter estimation. The focus on the right tail is particularly important in case of sub-daily durations (Wang et al., 2020; Marra et al., 2020).

We adopted the two parameter Weibull distribution for modelling the distribution of precipitation ordinary events, which has been applied in several other studies for daily and subdaily durations (e.g., Papalexiou et al., 2018; Marra et al., 2020) as well as in other applications over the analysed study area (e.g., Formetta et al. 2022, Dallan et al. 2022, 2023, 2024). The SMEV formulation presented in Eq. (1) therefore becomes an exponentiated Weibull:

$$G(x) = \left[1 - e^{-\left(\frac{x}{\lambda}\right)^{\kappa}}\right]^n \tag{2}$$

where $\lambda > 0[mmh^{-1}]$ is the scale parameter and $\kappa > 0$ [-] is the shape or tail parameter of the Weibull distribution and n is the average number of ordinary events in a year. Starting from 1 h continuous rainfall time series (obtained by aggregating the 5 min gauged rainfall data), we define as "storms" all the consecutive time intervals that include rainfall and are separated by dry intervals (<0.1 mm in each of the 1 h time intervals) of at least 24 h (e.g. Restrepo-Posada and Eagleson 1982, Tarolli et al. 2012). At each location, these storms can be interpreted as independent meteorological objects (see, Marra et al., 2020). "Ordinary events" of multiple durations are then computed for each storm by calculating the maximum intensity using a moving window of the duration of interest (Marra et al., 2020). In this study, we considered durations of 1, 3, 6, 12, and 24 h. Using this approach the parament n at a given location (Eq. (3)) represents the average number of storms per year and is, thus, the same of the number of ordinary events per year at all durations. As shown by Marra et al. (2020), this approach yields ordinary events that scale with duration in the same way as annual maxima.

3.2. Parameter estimation at ungauged locations

We compared two different methods for estimating extreme rainfall return levels at ungauged locations. One is more traditional and based on the rain gauge only, and one exploits the potential of combining rain gauge data and CPM model simulations. Both the approaches make use of two interpolation algorithms, one deterministic i.e. the inverse distance weighted (IDW) and one geostatistical i.e. the kriging with external drift (Garen et al., 1994, KED), to disentangle the eventual effect of including or not the elevation as covariate of the unknown variable.

The KED algorithm (Garen and Marks, 2005; Garen et al., 1994) includes the OK as particular cases. If the slope of the linear regression between the target and the secondary variable is statistically significant (p-value lower than 0.05) the KED exploits the potential of the secondary variable, otherwise an OK is performed on the target variable.

The station-based regionalization method (named using the acronym stat) is based on the following steps:

1. the estimation of the SMEV parameter set $\theta_{i,d}^{stat} = (\lambda_d, \kappa_d, n)$ for each ith gauged site and analysed rainfall duration d, i.e. 1, 3, 6, 12, and 24 h.
2. the interpolation of the estimated parameter set $\theta_{j,d}^{stat}$ in a generic ungauged location j; this is performed using the IDW and the KED spatialization methods.
3. the estimation of the return levels at the jth ungauged location, corresponding to assigned return periods ($T = 2$, 10, and 50 years), $q_{j,d,T}^{stat}\left[mm\ h^{-1}\right]$

The station-CPM integrated regionalization method (named using the acronym s-CPM) is based on the following steps:

1. the estimation of the SMEV parameter set $\theta_{i,d}^{stat}$ and $\theta_{k,d}^{cpm} = (\lambda_d, \kappa_d, n)$ for each duration d and for each ith gauged site and kth co-located pixel of the CPM domain, i.e. the nearest CPM grid point to the ith rain gauge (Dallan et al., 2023, 2024)
2. the computation of the bias (i.e. the ratio) between each parameter of the $\theta_{i,d}^{stat}$ and $\theta_{k,d}^{cpm}$ arrays;
3. the interpolation of the estimated bias for each of the three parameters in a generic ungauged location j; this is performed using both IDW and KED spatialization methods;
4. the bias correction of the $\theta_{j,d}^{cpm}$ using the interpolated bias computed at the point 3;
5. the estimation of the extreme return levels at the jth ungauged location $q_{j,d,T}^{s-cpm}\left[mm\ h^{-1}\right]$ using the bias corrected parameter set estimated at point 4.

We consider that the extreme rainfall distribution parameters estimated from CPM have a systematic and a random error component with respect to the unknown truth, of which the rainfall distribution parameters estimated from the raingauges is the best representation. By applying the s-CPM method we assume that the systematic error component is larger than the random one and we test this approach over different durations, return levels, and different station densities.

3.3. Evaluation of the return level estimation methods in ungauged locations

We start with a leave-one-out application in which we consider each of the available 174 rain gauges as ungauged and use other stations to estimate the relative information. To explore the influence of the station density on the prediction in ungauged locations provided by the two regionalization methods we then use: (i) all the remaining 173 rain gauges (corresponding to a station density of ~1/196 km^2), and randomly selected subsets of rain gauges corresponding to densities of (ii) 1/400 km^2 and 1/800 km^2.

The random sampling for the two lower densities is repeated 100 times for each "ungauged" station, to ensure a full statistical description of the errors at each location while reducing the effect of the random selection of the gauged stations (e.g. Miniussi and Marra 2021). In doing so, to avoid the formation of spatial clusters of randomly selected rain gauges, we enforce a minimum inter-distance between selected stations equal to half of the square root of the analysed densities (e.g., Nikolopoulos et al. 2015).

To assess the effectiveness of the presented methods and account for the 100 independent simulations, we computed for each station, rainfall duration d (i.e. 1, 3, 6, 12, and 24 h) and return period T (i.e. 2, 10, and 50 years) the fractional standard error across all the stations for a given method m and density $dens$ as:

$$e_{dens,m} = \frac{1}{q_{ref}} \cdot \sqrt{\sum_{i=1}^{NI} \left(q_{dens,m} - q_{ref}\right)^2} \tag{3}$$

where NI is the number of iterations, which is equal to 1 for the station density 1/196 km^2 and equal to 100 for station density 1/400 km^2 and 1/800 km^2; q_{ref} is the reference return level computed from the station data, and $q_{dens,m}$ is the rainfall return level computed with method m and density $dens$. To investigate the effect of the interpolation algorithm on the estimate of $q_{dens,m}$ we computed $e_{dens,m}$ both for the IDW and for the KED.

Finally, to quantify the improvement/deterioration of the mean fractional standard error across all duration of the interpolation methods (i.e. KED versus IDW) or regionalization methods (e.g. s-CPM versus stat) we consider the following index:

$$i_T = 100 \cdot \frac{f\left(e_{d,stat}^{proposed}\right) - f\left(e_{d,stat}^{reference}\right)}{f\left(e_{d,stat}^{reference}\right)} \tag{4}$$

where f indicates in turn the mean and the interquartile range of the fractional standard errors of the reference (IDW and stat, respectively) and the proposed methods (stat and s-CPM, respectively) across all the durations, for a given return period. Negative (positive) values of i_T indicates that the proposed method shows an improvement (deterioration) in accuracy with respect to the reference method, being $f\left(e_{d,stat}^{proposed}\right)$ lower (higher) than $f\left(e_{d,stat}^{reference}\right)$.

4. Results

4.1. Assessment of the interpolation methods for the highest station density scenario

For the highest station density (i.e. 1/196 km^2) we assessed which interpolation algorithm (IDW or KED) provides the most accurate prediction across all the durations and analysed return period (see Fig. 2), for both stat and s-CPM regionalization methods. The KED algorithm, which also includes the information on the orography effect in the interpolation process, shows an average reduction of the mean fractional standard error (across all durations) of 16 %, 15 %, and 12 % (2-year

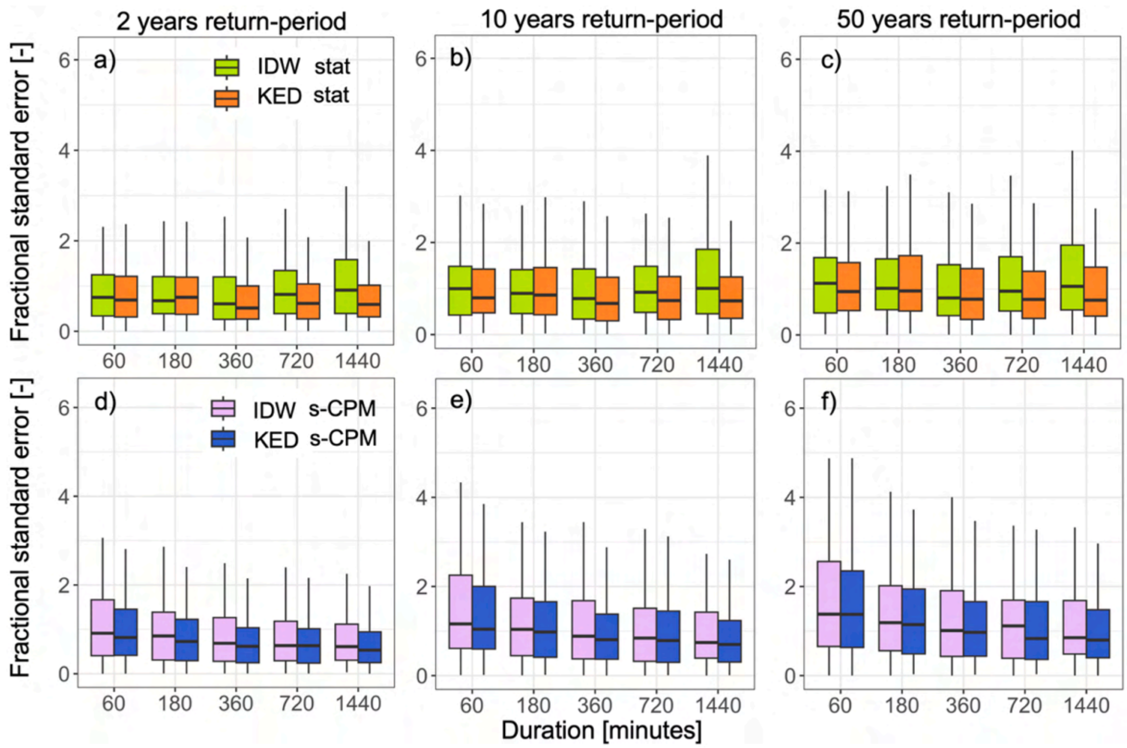

Fig. 2. Boxplot of the fractional standard error for the station density 1/196 km^2, for the stat (a–c) and the s-CPM (d–f) method across all the analyzed durations and return periods, grouped by interpolation algorithms (IDW and KED).

return levels) and 11 %, 7 %, and 4 % (50-year return level) compared to the IDW algorithm. For the three analysed return periods and for the stat (s-CPM) regionalization methods, the KED algorithm also provides a reduction of the interquartile range of the fractional standard error, on average across all the durations, of 11 %, 7 %, 5 % (20 %, 16 %, 8 %), respectively. We therefore choose to use the KED interpolation algorithm to test the effectiveness of the two methods for predicting return levels in ungauged locations (i.e. stat and s-CPM).

4.2. Return level estimation in ungauged locations with varying station density

Results in Fig. 3 show the boxplot of the fractional standard error computed in each station for different durations, for the two regionalization methods (s-CPM and stat) together with the sampling (stochastic) uncertainty. The latter has been quantified using a 1000-iteration bootstrap resampling procedure with replacement on the years (e.g. Efron and Tibshirani 1994, Overeem et al. 2008).

Results are organized by return period (2, 10, and 50 years) and by station density (1/196 km^2, 1/400 km^2 and 1/800 km^2) to investigate how the performances of the methods vary while the monitoring network becomes significantly sparser.

Results for the highest station density (1/196 km^2) show that the KED stat outperforms the KED s-CPM especially for short durations (lower than 6 h) and toward longer return periods. For longer duration the average performance of the two methods are comparable. Overall, on average across all the durations (see Table 1), the KED s-CPM method provides an 8 % reduction of the mean fractional standard error with respect the KED stat for 2 years return period (Fig. 3-a) while providing an increasing of 2.5 % and 8 % for return periods of 10 and 50 years (Fig. 3-e and h), respectively.

Results for the lower station densities (1/400 and 1/800 km^2) show that the KED s-CPM outperforms the traditional KED stat method. This is particularly true for return periods of 2 and 10 years and while moving towards long durations (longer than 3–6 h for 1/400 km^2 and longer than 3 h for 1/800 km^2).

Table 1 shows that KED s-CPM method for station density 1/400 km^2 provides, on average across all the durations, a reduction of the mean fractional standard error with respect to the traditional KED stat method of 16 %, 8 % and 3 %, while moving from 2 to 50 years return period. The performances of KED s-CPM are comparatively better for station density 1/800 km^2, with a reduction of 25 %, 13 % and 8 %, for the three return periods.

We then disentangled the effect played by the elevation on the performance of the two methods. Fig. 4 shows the boxplot of the fractional standard error computed in each station for different durations, for the two regionalization methods (s-CPM and stat) and the uncertainty due to the sampling uncertainty, for different durations and 10 years return period organized by equi-populated elevation classes.

Results for the highest station density (1/196 km^2) show that the KED s-CPM outperforms the KED stat especially for durations longer than 3 h, moving towards higher elevation (above 150 m). For the lower station densities (1/400 and 1/800 km^2) KED s-CPM outperforms the traditional KED stat method generally across all the durations for elevations above 150 m. For lower elevations it outperforms KED stat only for 24 h durations for station density of 1/400 km^2 and for durations longer than 6 h for station density of 1/800 km^2. On average across all durations (Table 2), for the highest station density case (1/196 km^2), the traditional KED stat clearly outperforms KED s-CPM for elevations lower than 150 m. For elevations higher than 150 m, KED s-CPM equalizes or improves the mean fractional standard error value with respect to KED stat, particularly at the elevation band 150–700 m. Results for the lowest station density 1/800 km^2 show that on average across all the durations, the KED s-CPM method reduces the mean fractional standard error for elevations class, with remarkable performances for elevation higher than 150 m. Intermediate results are reported for the intermediate density (1/400 km^2).

Finally, Figs. 5 and 6 show the maps of the interpolated rainfall intensities for 1 h and 24 h duration, respectively, and for 2 and 50 years return period, obtained using the KED-stat and KED s-CPM

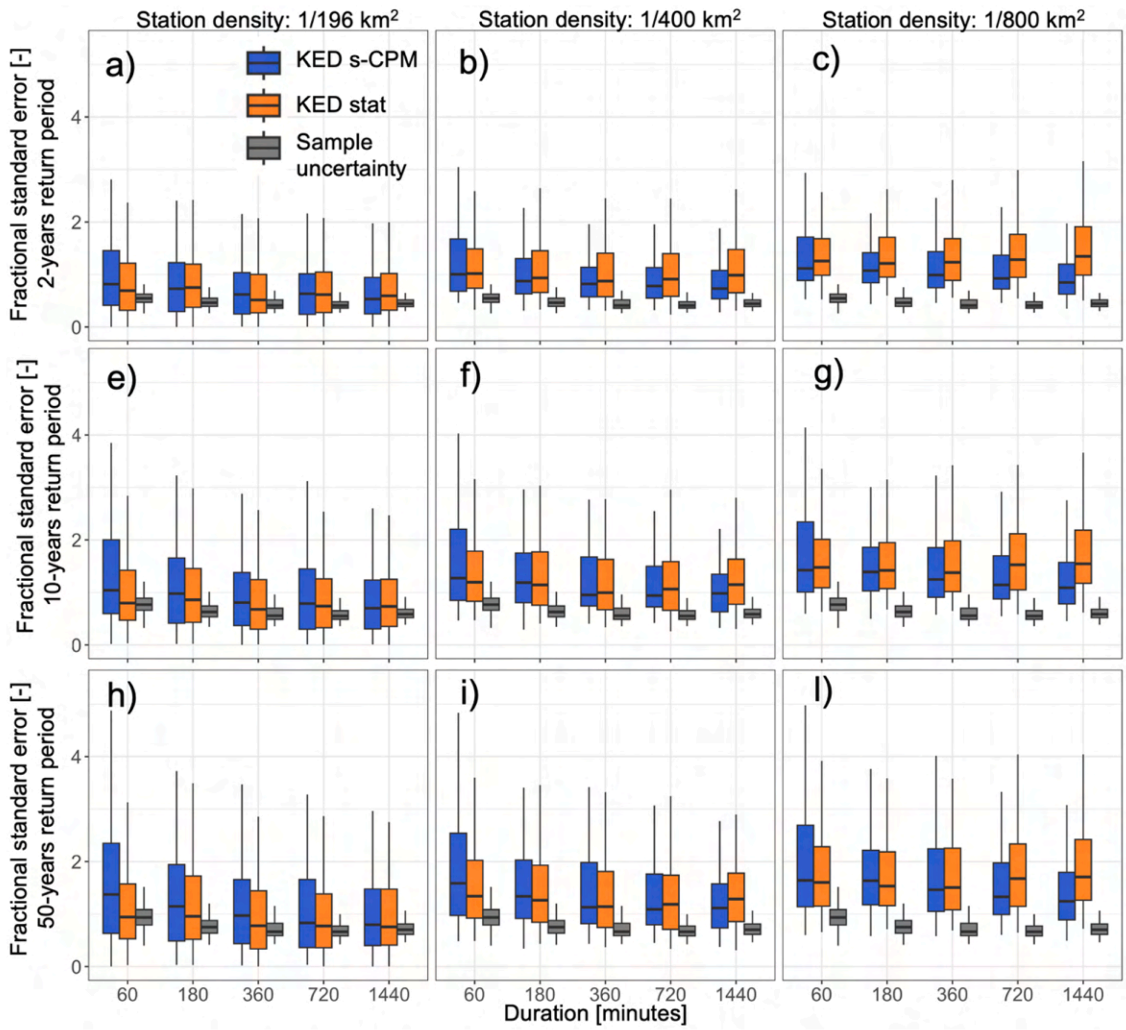

Fig. 3. Boxplot of the fractional standard error for the different station densities (1/196 km^2, 1/400 km^2 and 1/400 km^2), different return periods, i.e. 2 (a–c), 10 (e–g), and 50 years (h, i, l), and different durations organized by regionalization method, i.e. stat in orange and s-CPM in blue. In grey the boxplot of the sample uncertainty is reported, which is estimated considering the station as gauged and summaries the uncertainty due the sample randomness.

Table 1
Percentage of improvement (if negative) or deterioration (if positive) of the mean value of the fractional standard error of the s-CPM over the stat method, across all the stations, durations and organized by return periods (rows) and station density (columns).

	Station density		
	1/196 km^2	1/400 km^2	1/800 km^2
2 years return period	−8.0	−16.3	−24.6
10 years return period	2.5	−8.5	−13.3
50 years return period	8.0	−3.2	−8.3

regionalization methods and the corresponding fractional bias (computed as the ratio of the differences between return levels estimated by s-CPM and stat to mean of the two). At 1 h, the KED-stat maps (Fig. 5a–d) show the so called "reverse orographic effect" (Avanzi et al., 2015; Formetta et al., 2022; Dallan et al., 2023), with intensity decreasing with increasing elevation. The overall pattern is also well represented by the KED s-CPM maps (Fig. 5b–e), even though in a less marked way. At 24 h duration (Fig. 6), both maps show a direct orographic effect (or orographic enhancement), with intensity generally slightly increasing with elevation, but also showing a reduced intensity corresponding to the high elevation north-west portion, due to the orographic shielding offered by the surrounding mountain ranges. On the other side, results for the KED s-CPM method at 1 h duration (Fig. 5-b and e) seem much scattered compared to the KED stat (Fig. 5-a and d) and to the 24 h duration (Fig. 6-b and -e).

The fractional bias increases with return period for both 1- and 24 h durations, with the KED s-CPM return levels being higher than the KED stat in the mountain areas and lower in the valleys for the 1 h durations (Fig. 5-c and f). The spatial pattern of the fractional bias for 24 h duration is less clear, with KED s-CPM return levels being lower than KED stat in limited areas in the north-western and north-eastern part and higher in small portions of the central part of the study area.

5. Discussion

The KED method, which includes the elevation as additional information in the interpolation, outperformed the traditional IDW approach, for both regionalization methods based on rain gauges only (stat) and on rain gauges combined with CPM simulations (s-CPM). This agrees with other studies which performed interpolation of extreme rainfall in orographically complex regions. Haberlandt (2007), for instance, in a spatial estimation analysis of hourly heavy rainfall events in Germany, successfully explored the use of radar based and daily rainfall precipitation, together with elevation. Page et al. (2022) tested different co-variates for inclusion into the interpolation process, finding a smoothed elevation to be the most appropriate. On the other hand,

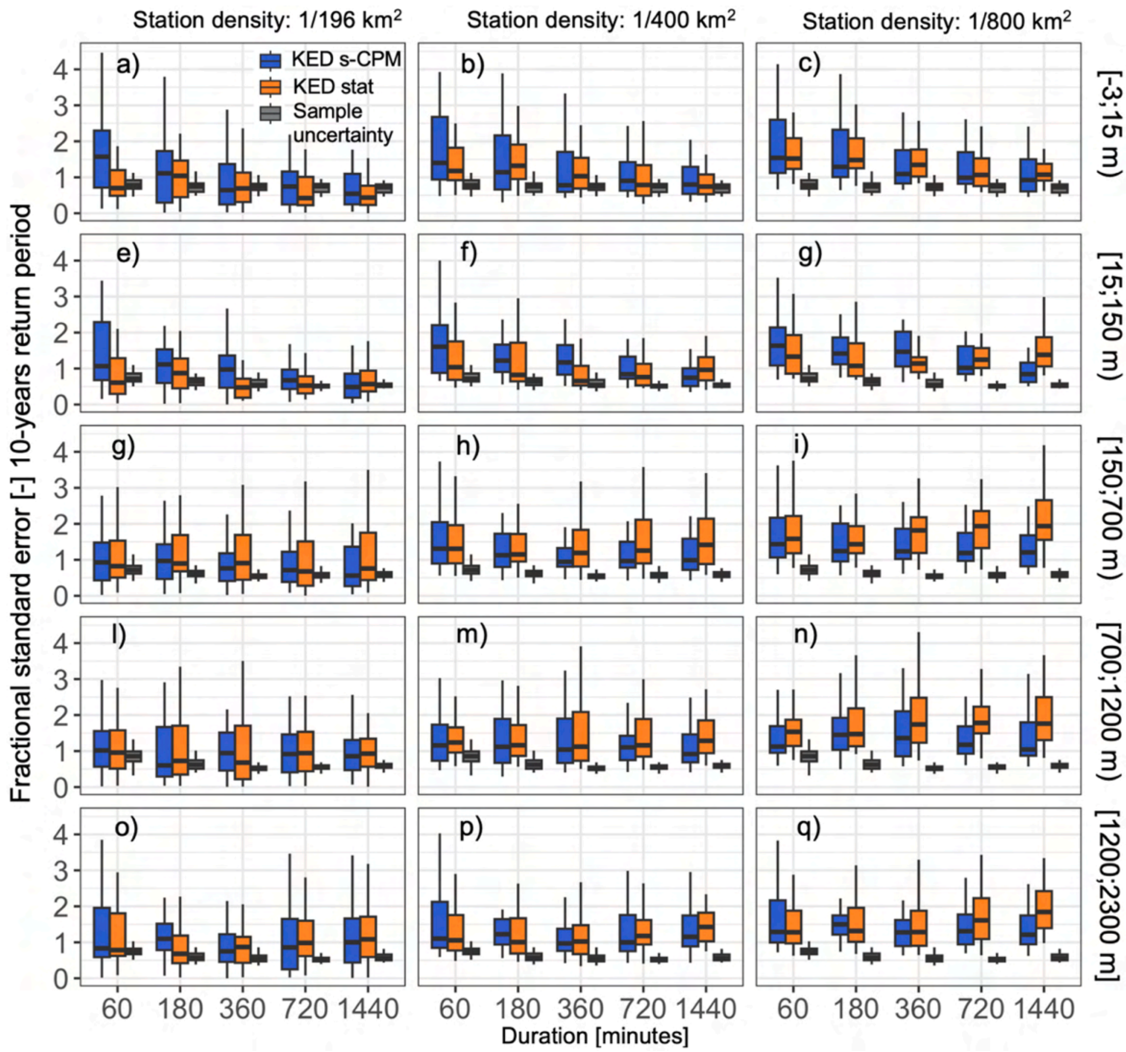

Fig. 4. Boxplot of the fractional standard error for the different station densities (1/196 km^2, 1/400 km^2 and 1/400 km^2), for the 10 years return period, and different durations organized by regionalization method, i.e. stat in orange and s-CPM in blue. In grey the boxplot of the sample uncertainty is reported, which is estimated considering the station as gauged and summaries the uncertainty due the sample randomness. Results are grouped by classes of elevation bands (indicated on the right-hand side of each row).

Table 2
Percentage of improvement (if negative) or deterioration (if positive) of the mean value of the fractional standard error of the s-CPM over the stat method across all the stations, durations, and for the 10 years return period organized by elevation bands and station density (columns).

	Station density		
	1/196 km^2	1/400 km^2	1/800 km^2
−3;15	33.9	7.3	−4.5
15;150	40.5	9.8	−1.8
150;700	−17.8	−18.2	−25.9
700;1200	−7.7	−12.6	−26.2
1200;2300	3.0	−2.6	−6.2

Minuissi and Marra (2021) interpolated daily extreme rainfall return levels over Germany by spatially estimating the SMEV at-site parameters testing the nearest neighbour, the IDW and the Ordinary Kriging methods and finding the IDW as the algorithm providing the more accurate estimates. We show here that it is possible to improve over their findings by accounting for the elevation information in the interpolating process using the KED method.

We extend the work of Poschlod and Koh (2024) by exploring the potential of combining CPM sub-daily rainfall field simulation and at site sub-daily rainfall measurements to estimate moderate to extreme rainfall return levels. Given the structure of the tested methods, the results reflect the contrast between the spatial variability of the three distribution parameter bias fields (which are interpolated by the s-CPM procedure) and that of the three distribution parameter fields (which are interpolated by the stat procedure). The biases in the distribution parameters and return levels were assessed for different durations by Dallan et al. (2023, 2024), who reported larger biases at 1 h, decreasing with increasing the rainfall duration. These authors also discussed the physical reasons for these biases. The significant biases in the distribution parameters were generally found in the lowlands along the coast, and in limited areas at high elevation. Conversely, mid elevation areas showed generally not significant biases. This highlights some CPM limitations in simulating the high dynamical interacting processes between large-scale atmospheric systems and local-scale processes, which generate extreme rainfall events in flat/coastal areas (e.g., Adinolfi et al. 2023, Dallan et al. 2023) and in some high elevation areas. As can be noted from Dallan et al. (2024), the higher the bias the larger also its spatial variability. They found biases on return levels (which translate to distribution parameter biases) with higher magnitude and a bigger spatial variability at 1 h duration, decreasing with longer durations,

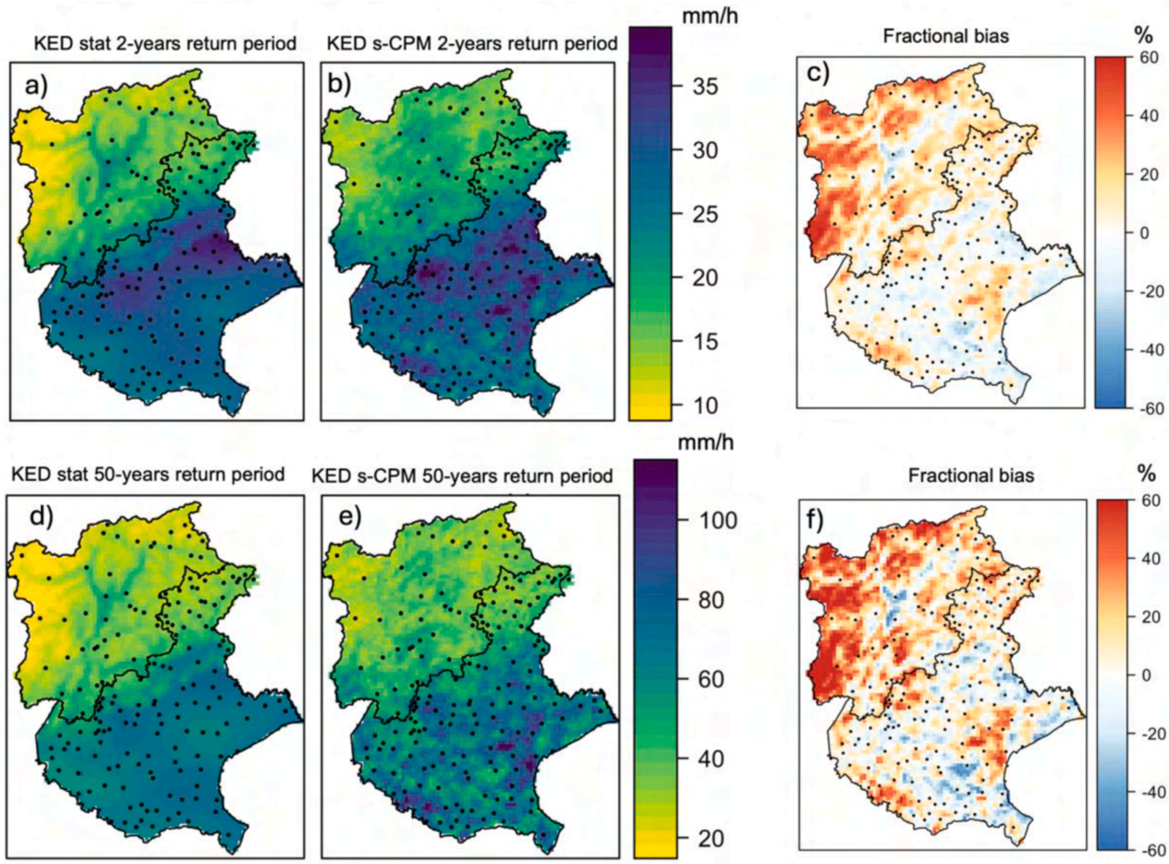

Fig. 5. 1 h duration rainfall intensities for 2 and 50 years return period and fractional bias (i.e. ratio of the differences between return levels estimated by s-CPM and stat to mean of the two) in percentage for the KED stat (a–c) and KED s-CPM (b and d) regionalization methods.

with the 24 h exhibiting biases smoothed in magnitude and spatially more uniform. These considerations can explain the noisier patterns of the return levels at 1 h for the s-CPM method, and its increasing performances with increasing duration. Also, in Dallan et al. (2023), comparatively more important and spatially variable biases were found for the shape parameter. This explains why the performances of the s-CPM method decreases with increasing the return period, a characteristic which is mainly controlled by the shape parameter.

Given this background, it is not surprising that at 24 h KED s-CPM increases the accuracy of the extreme rainfall return levels prediction in ungauged locations with respect to KED stat. This result agrees with the findings of Poschlod and Koh (2024) in Germany. Furthermore, we showed that this improvement is also evident for sub-daily durations and increases with decreasing the station densities. Symmetrically with the relevance of the biases in the distribution parameters, and as an average across all the durations, the added value of the KED s-CPM method is generally more evident for medium high elevations (from 150 m to 1200 m). This improvement is still observed for high elevations (from 1200 m to 2300 m), even though the added value is here less conspicuous. For low elevation (i.e. −3 m to 150 m) the improvement is absent for station density of 1/400 km^2 or minimum (i.e. less than 6 %) for station densities of 1/800 km^2.

Results showed that for: (i) long durations only (12 and 24 h) in the highest station density case and (ii) all the analyzed durations in the lower station density cases the hypotheses assumed by the s-CPM method holds, i.e. the systematic error component in the estimated parameters from CPM rainfall with respect the parameters estimated from raingauge data is larger than the random error component. The opposite occurs for short durations (1, 3 and 6 h) in the highest station density case, where the random component is larger, and the s-CPM method does not provide added value in the estimation of extreme rainfall with respect to the traditional Stat method in our study area.

The KED method provides the uncertainty related to the estimated parameters of the SMEV distribution under the assumption of Gaussian errors. Moving from this estimated uncertainty towards the uncertainty in the return level is not an easy task, that would require strict and unverified hypotheses on the independence of the error in the distribution parameters. A formal propagation of these errors could only be done for each parameter independently, for example using Taylor series as done in Siena et al. (2023). However, the formal estimation and propagation of the prediction uncertainty is not an objective of this paper.

We recognize that epistemic uncertainty is associated with our choice of a two parameter Weibull distribution. Despite this, the limited record length of the CPM simulations requires using methods that are different from the traditional ones. This Weibull model, however, is supported by atmospheric physics (WIlson and Toumi, 2005), empirical observations (Marra et al., 2023), previous studies (Zorzetto et al., 2016, Schellander et al., 2019) and stochastic modeling results (Papalexiou et al., 2022).

Finally, it should be noted that the stat and the s-CPM method are based on the availability of different record lengths. On the one hand the stat method is executed by using rainfall record lengths ranging from 14 to 37 years, on the other hand the s-CPM method is based on just 10 years data, as it is limited by the CPM temporal availability. While this choice ensures that the reference return levels are characterised by the lowest possible sampling uncertainty, it also means that the comparison factorises different sampling uncertainties, thus penalising the s-CPM method that has higher sampling uncertainties.

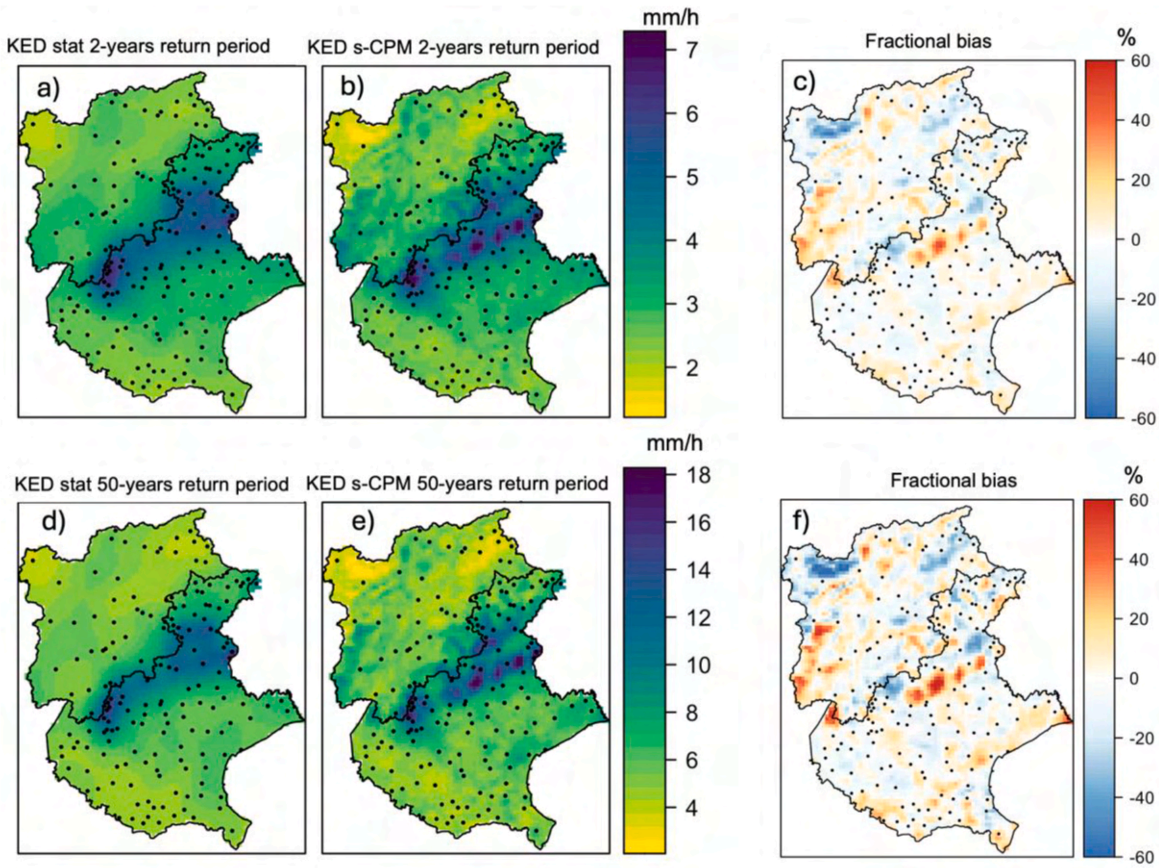

Fig. 6. 24 h duration rainfall intensities for 2 and 50 years return period and fractional bias (i.e. ratio of the differences between return levels estimated by s-CPM and stat to mean of the two) in percentage for the KED stat (a–c) and KED s-CPM (b and d) regionalization methods.

6. Conclusions

In this paper we quantified the added values provided by CPM simulated rainfall field in combination with raingauge data in estimating sub-daily extreme rainfall return levels in ungauged locations. To overcome limitations due to the short record of CPM simulations, we used a non-asymptotic framework (SMEV) for estimating moderate-to-extreme rainfall return levels. We also quantified the influence: i) of the interpolation algorithms, by comparing two of the most used, i.e. KED and IDW and ii) of varying station densities on the regionalization of extreme rainfall in ungauged locations.

The KED interpolation method outperforms the traditional IDW for both the stat and the s-CPM regionalisation methods, with a reduction of the mean fractional standard error of 16 %, 15 %, and 12 % (for the stat) and 11 %, 7 %, and 4 % (for the s-CPM) across the three analysed return periods (2, 10, and 50 years) and on average across all the durations.

The added value of CPM simulations to derive sub-daily return levels depends on the station density and on the duration of interest. For the highest station density (1/196 km^2) the traditional method outperforms the CPM informed regionalization method for short durations (lower than 6 h). For longer durations, the performances of the two methods are comparable.

In scenarios with lower station densities (1/400 and 1/800 km^2), the CPM informed estimates outperform the traditional interpolation. For the lowest station density, the reduction of the mean fractional standard error (on average across durations) amounts to 24 %, 13 % and 8 % for 2, 10, and 50 years return period respectively. For the intermediate density, the reduction is comparatively lower and amounts to 16 %, 8 % and 3 %, respectively. Finally, results are discussed in terms of elevation. The highest improvements of the CPM informed regionalization methods are observed in medium high/high elevations.

The flexibility of the proposed regionalization method and the peculiarity of the analyzed study area (which cover a variety of climate, spanning from coastal environments to high elevation alpine zones) show how the approach can be extended for analysis in different climates and eventually to different climatological variables. Future efforts should focus on using ensembles of convection-permitting model simulations. The use of multiple models could decrease the biases and the sampling uncertainties, thereby improving the representation of high temporal resolution extreme rainfall. Additionally, long-term CPM simulations could be used to reduce the uncertainty of the applied extreme value distribution framework.

CRediT authorship contribution statement

Giuseppe Formetta: Conceptualization, Methodology, Software, Writing – original draft, Data curation, Formal analysis. **Eleonora Dallan:** Data curation, Methodology, Software, Writing – review & editing. **Marco Borga:** Supervision, Investigation, Conceptualization, Methodology, Writing – review & editing. **Francesco Marra:** Conceptualization, Methodology, Writing – review & editing.

Declaration of competing interest

The authors declare that they have no known competing financial interests or personal relationships that could have appeared to influence the work reported in this paper.

Financial support

This research has been supported by the Fondazione Cassa di Risparmio di Padova e Rovigo (Excellence Grant 2021 to the Resilience

Project). This study has also been carried out within the RETURN Extended Partnership and received funding from the European Union Next-GenerationEU (National Recovery and Resilience Plan – NRRP, Mission 4, Component 2, Investment 1.3 – D. D. 1243 2/8/20). This work was partially supported by the INTENSE project (raINfall exTremEs and their impacts: from the local to the National ScalE) funded by the European Union - Next Generation EU in the framework of PRIN (Progetti di ricerca di Rilevante Interesse Nazionale) programme (grant 2022ZC2522). GF was partially funded by Coach-Wat "PRIN 2022″ (Progetti di ricerca di Rilevante Interesse Nazionale), identification code 2022FXJ3NN_001 - CUP E53D23004390001.

Acknowledgments

The authors acknowledge the institutes providing observational data: Provincia Autonoma di Trento, Provincia Autonoma di Bolzano, and Agenzia Regionale per la Prevenzione e Protezione Ambientale del Veneto. The authors gratefully acknowledge the WCRP-CORDEX-FPS on Convective phenomena at high resolution over Europe and the Mediterranean (FPSCONVALP-3) and in particular ETH Zurich for sharing the climate model data.

Data availability

Data will be made available on request.

References

Adhikary, P.P., Dash, C.J., 2017. Comparison of deterministic and stochastic methods to predict spatial variation of groundwater depth. Appl. Water Sci. 7, 339–348.

Adinolfi, M., Raffa, M., Reder, A., Mercogliano, P., 2023. Investigation on potential and limitations of ERA5 Reanalysis downscaled on Italy by a convection-permitting model. Clim. Dyn. 61 (9), 4319–4342.

Avanzi, F., De Michele, C., Gabriele, S., Ghezzi, A., Rosso, R., 2015. Orographic signature on extreme precipitation of short durations. J. Hydrometeorol. 16 (1), 278–294.

Ban, N., Rajczak, J., Schmidli, J., Schär, C., 2020. Analysis of Alpine precipitation extremes using generalized extreme value theory in convection-resolving climate simulations. Clim. Dyn. 55 (1), 61–75.

Ban, N., Schmidli, J., Schär, C., 2014. Evaluation of the convection-resolving regional climate modeling approach in decade-long simulations. J. Geophys. Res. Atmos. 119 (13), 7889–7907.

Berndt, C., Haberlandt, U., 2018. Spatial interpolation of climate variables in Northern Germany—Influence of temporal resolution and network density. J. Hydrol. Reg. Stud. 15, 184–202. https://doi.org/10.1016/j.ejrh.2018.02.002.

Berthou, S., Kendon, E.J., Chan, S.C., Ban, N., Leutwyler, D., Schär, C., Fosser, G., 2020. Pan-European climate at convection-permitting scale: a model intercomparison study. Clim. Dyn. 55, 35–59.

Blöschl, G., Bierkens, M.F., Chambel, A., Cudennec, C., Destouni, G., Fiori, A., Renner, M., 2019. Twenty-three unsolved problems in hydrology (UPH)–a community perspective. Hydrol. Sci. J. 64 (10), 1141–1158.

Brotzge, J.A., Berchoff, D., Carlis, D.L., Carr, F.H., Carr, R.H., Gerth, J.J., Wang, X., 2023. Challenges and opportunities in numerical weather prediction. Bull. Am. Meteorol. Soc. 104 (3), E698–E705.

Ceresetti, D., Ursu, E., Carreau, J., Anquetin, S., Creutin, J.D., Gardes, L., Girard, S., Molinie, G., 2012. Evaluation of classical spatial-analysis schemes of extreme rainfall. Nat. Hazards Earth Syst. Sci. 12 (11), 3229–3240.

Claps, P., Ganora, D., Mazzoglio, P., 2022. Rainfall regionalization techniques. Rainfall. Elsevier, pp. 327–350.

Coppola, E., Sobolowski, S., Pichelli, E., Raffaele, F., Ahrens, B., Anders, I., Warrach-Sagi, K., 2020. A first-of-its-kind multi-model convection permitting ensemble for investigating convective phenomena over Europe and the Mediterranean. Clim. Dyn. 55, 3–34.

Dallan, E., Borga, M., Zaramella, M., Marra, F., 2022. Enhanced summer convection explains observed trends in extreme subdaily precipitation in the Eastern Italian Alps. Geophys. Res. Lett. 49 (5), e2021GL096727.

Dallan, E., Marra, F., Fosser, G., Marani, M., Formetta, G., Schär, C., Borga, M., 2023. How well does a convection-permitting regional climate model represent the reverse orographic effect of extreme hourly precipitation? Hydrol. Earth Syst. Sci. 27 (5), 1133–1149.

Dallan, E., Borga, M., Fosser, G., Canale, A., Roghani, B., Marani, M., Marra, F., 2024. A method to assess and explain changes in sub-daily precipitation return levels from convection-permitting simulations. Water Resour. Res. 60. https://doi.org/10.1029/2023WR035969 e2023WR035969.

Das, S., Zhu, D., Yin, Y., 2020. Comparison of mapping approaches for estimating extreme precipitation of any return period at ungauged locations. Stochastic Environ. Res. Risk Assess. 34 (8), 1175–1196.

Dee, D.P., Uppala, S.M., Simmons, A.J., Berrisford, P., Poli, P., Kobayashi, S., Andrae, U., Balmaseda, M.A., Balsamo, G., Bauer, P., Bechtold, P., Beljaars, A.C.M., van de Berg, L., Bidlot, J., Bormann, N., Delsol, C., Dragani, R., Fuentes, M., Geer, A.J., Haimberger, L., Healy, S.B., Hersbach, H., Hólm, E.V., Isaksen, L., Kållberg, P., Köhler, M., Matricardi, M., McNally, A.P., Monge-Sanz, B.M., Morcrette, J.-J., Park, B.-K., Peubey, C., de Rosnay, P., Tavolato, C., Thépaut, J.-N., Vitart, F., 2011. The ERA-Interim reanalysis: configuration and performance of the data assimilation system. Q. J. R. Meteorol. Soc. 137 (656), 553–597.

Efron, Bradley, Tibshirani, Robert J., 1994. *An* Introduction to the Bootstrap. Chapman and Hall/CRC.

Faulkner, D.S., Prudhomme, C., 1998. Mapping an index of extreme rainfall across the UK. Hydrol. Earth Syst. Sci. 2, 183–194. https://doi.org/10.5194/hess-2-183-1998.

Fliri, F., 1975. Das klima der Alpen im raume von Tirol, München : Universitätsverlag Wagner, 1975. ISBN: 3703000090.

Formetta, G., Feyen, L., 2019. Empirical evidence of declining global vulnerability to climate-related hazards. Glob. Environ. Change 57, 101920.

Formetta, G., Marra, F., Dallan, E., Zaramella, M., Borga, M., 2022. Differential orographic impact on sub-hourly, hourly, and daily extreme precipitation. Adv. Water Resour. 159, 104085.

Fosser, G.S.K.P.B., Khodayar, S., Berg, P., 2015. Benefit of convection permitting climate model simulations in the representation of convective precipitation. Clim. Dyn. 44, 45–60.

Garen, D.C., Johnson, G.L., Hanson, C.L., 1994. Mean areal precipitation for daily hydrologic modeling in mountainous regions 1. JAWRA J. Am. Water Resour. Assoc. 30 (3), 481–491.

Garen, D.C., Marks, D., 2005. Spatially distributed energy balance snowmelt modelling in a mountainous river basin: estimation of meteorological inputs and verification of model results. J. Hydrol. 315 (1–4), 126–153.

Giorgi, F., 2019. Thirty years of regional climate modeling: where are we and where are we going next? J. Geophys. Res. Atmos. 124 (11), 5696–5723.

Goovaerts, P. (1997). Geostatistics for natural resources evaluation. Applied Geostatistics.

Haberlandt, U., 2007. Geostatistical interpolation of hourly precipitation from rain gauges and radar for a large-scale extreme rainfall event. J. Hydrol. 332 (1–2), 144–157.

Hosking, J.R.M., & Wallis, J.R. (1997). Regional frequency analysis (p. 240).

Hosseini, V.R., Shivanian, E., Chen, W., 2016. Local radial point interpolation (MLRPI) method for solving time fractional diffusion-wave equation with damping. J. Comput. Phys. 312, 307–332.

Hydrology, Institute of, 1999. Flood Estimation Handbook. Centre for Ecology & Hydrology, Wallingford, UK (five volumes).

Isotta, F.A., Frei, C., Weilguni, V., Perčec Tadić, M., Lassegues, P., Rudolf, B., Pavan, V., Cacciamani, C., Antolini, G., Ratto, S.M., Munari, M., Micheletti, S., Bonati, V., Lussana, C., Ronchi, C., Panettieri, E., Marigo, G., Vertačnik, G., 2014. The climate of daily precipitation in the Alps: development and analysis of a high-resolution grid dataset from pan-Alpine rain-gauge data. Int. J. Climatol. 34 (5), 1657–1675.

Jalbert, J., Genest, C., Perreault, L., 2022. Interpolation of precipitation extremes on a large domain toward idf curve construction at unmonitored locations. J. Agric. Biol. Environ. Stat. 27 (3), 461–486.

Kendon, E.J., Ban, N., Roberts, N.M., Fowler, H.J., Roberts, M.J., Chan, S.C., Wilkinson, J.M., 2017. Do convection-permitting regional climate models improve projections of future precipitation change? Bull. Am. Meteorol. Soc. 98 (1), 79–93.

Kendon, E.J., Roberts, N.M., Senior, C.A., Roberts, M.J., 2012. Realism of rainfall in a very high-resolution regional climate model. J. Clim. 25 (17), 5791–5806.

Kidd, C., Becker, A., Huffman, G.J., Muller, C.L., Joe, P., Skofronick-Jackson, G., Kirschbaum, D.B., 2017. So, how much of the Earth's surface is covered by rain gauges? Bull. Am. Meteorol. Soc. 98 (1), 69–78.

Knist, S., Goergen, K., Simmer, C., 2020. Effects of land surface inhomogeneity on convection-permitting WRF simulations over central Europe. Meteorol. Atmos. Phys. 132 (1), 53–69.

Lengfeld, K., Kirstetter, P.-E., Fowler, H.J., Yu, J., Becker, A., Flamig, Z., Gourley, J.J., 2020. Use of radar data for characterizing extreme precipitation at fine scales and short durations. Environ. Res. Lett. 15, 085003. https://doi.org/10.1088/1748-9326/ab98b4.

Marani, M., Ignaccolo, M., 2015. A metastatistical approach to rainfall extremes. Adv. Water Resour. 79, 121–126.

Marra, F., Armon, M., Borga, M., Morin, E., 2021. Orographic effect on extreme precipitation statistics peaks at hourly time scales. Geophys. Res. Lett. 48 (5), e2020GL091498.

Marra, F., Borga, M., Morin, E., 2020. A unified framework for extreme subdaily precipitation frequency analyses based on ordinary events. Geophys. Res. Lett. 47 (18), e2020GL090209.

Marra, F., Zoccatelli, D., Armon, M., Morin, E., 2019. A simplified MEV formulation to model extremes emerging from multiple nonstationary underlying processes. Adv. Water Resour. 127, 280–290.

Miniussi, A., Marra, F., 2021. Estimation of extreme daily precipitation return levels at-site and in ungauged locations using the simplified MEV approach. J. Hydrol. 603, 126946.

Nikolopoulos, E.I., Borga, M., Marra, F., Crema, S., Marchi, L., 2015. Debris flows in the eastern Italian Alps: seasonality and atmospheric circulation patterns. Nat. Hazards Earth Syst. Sci. 15 (3), 647–656.

Overeem, A., Buishand, A., Holleman, I., 2008. Rainfall depth-duration-frequency curves and their uncertainties. J. Hydrol. 348 (1–2), 124–134.

Ozkaya, A., 2023. Assessing the numerical weather prediction (NWP) model in estimating extreme rainfall events: a case study for severe floods in the southwest Mediterranean region, Turkey. J. Earth Syst. Sci. 132 (3), 125.

Page, T., Beven, K.J., Hankin, B., Chappell, N.A., 2022. Interpolation of rainfall observations during extreme rainfall events in complex mountainous terrain. Hydrol. Process. 36 (11), e14758.

Papalexiou, S.M., AghaKouchak, A., Foufoula-Georgiou, E., 2018. A diagnostic framework for understanding climatology of tails of hourly precipitation extremes in the United States. Water Resour. Res. 54 (9), 6725–6738.

Pellicone, G., Caloiero, T., Modica, G., Guagliardi, I., 2018. Application of several spatial interpolation techniques to monthly rainfall data in the Calabria region (southern Italy). Int. J. Climatol. 38 (9), 3651–3666.

Poschlod, B., 2021. Using high-resolution regional climate models to estimate return levels of daily extreme precipitation over Bavaria. Nat. Hazards Earth Syst. Sci. 21 (11), 3573–3598.

Poschlod, B., Koh, J., 2024. Convection-permitting climate models can support observations to generate rainfall return levels. Water Resour. Res. 60 (4) e2023WR035159.

Restrepo-Posada, P.J., Eagleson, P.S., 1982. Identification of independent rainstorms. J. Hydrol. 55 (1–4), 303–319.

Rockel, B., Will, A., Hense, A., 2008. The regional climate model COSMO-CLM (CCLM). Meteorol. Z. 17 (4), 347.

Schellander, H., Lieb, A., Hell, T., 2019. Error structure of metastatistical and generalized extreme value distributions for modeling extreme rainfall in Austria. Earth Space Sci. 6 (9), 1616–1632.

Shepard, D., 1968. A two-dimensional interpolation function for irregularly-spaced data. In: Proceedings of the 1968 23rd ACM National Conference, pp. 517–524.

Shmilovitz, Y., Marra, F., Enzel, Y., Morin, E., Armon, M., Matmon, A., Haviv, I., 2023. The impact of extreme rainstorms on escarpment morphology in arid areas: insights from the central Negev Desert. J. Geophys. Res. Earth Surf. 128 (10) e2023JF007093.

Siena, M., Levizzani, V., Marra, F., 2023. A method to derive satellite-based extreme precipitation return levels in poorly gauged areas. J. Hydrol. 626, 130295.

Sivapalan, M., Takeuchi, K., Franks, S.W., Gupta, V.K., Karambiri, H., Lakshmi, V., Zehe, E., 2003. IAHS Decade on Predictions in Ungauged Basins (PUB), 2003–2012: shaping an exciting future for the hydrological sciences. Hydrol. Sci. J. 48 (6), 857–880.

Sun, J., Xue, M., Wilson, J.W., Zawadzki, I., Ballard, S.P., Onvlee-Hooimeyer, J., Pinto, J., 2014. Use of NWP for nowcasting convective precipitation: recent progress and challenges. Bull. Am. Meteorol. Soc. 95 (3), 409–426.

Szolgay, J., Parajka, J., Kohnová, S., Hlavčová, K., 2009. Comparison of mapping approaches of design annual maximum daily precipitation. Atmos. Res. 92 (3), 289–307.

Tabios III, G.Q., Salas, J.D, 1985. A comparative analysis of techniques for spatial interpolation of precipitation 1. JAWRA J. Am. Water Resour. Assoc. 21 (3), 365–380.

Tarolli, P., Borga, M., Morin, E., Delrieu, G., 2012. Analysis of flash flood regimes in the North-Western and South-Eastern Mediterranean regions. Nat. Hazards Earth Syst. Sci. 12 (5), 1255–1265.

Thiessen, A.H., 1911. Precipitation averages for large areas. Mon. Weather Rev. 39 (7), 1082–1089.

Towler, E., Llewellyn, D., Prein, A., Gilleland, E., 2020. Extreme-value analysis for the characterization of extremes in water resources: a generalized workflow and case study on New Mexico monsoon precipitation. Weather Clim. Extremes 29, 100260.

UNSIDR, 2015. Sendai framework for disaster risk reduction 2015 - 2030. Technical Report, p. 37, URL: https://www.undrr.org/publication/sendai-framework-disaster-risk-reduction-2015-2030.

Wang, L., Marra, F., & Onof, C., 2020. Modelling sub-hourly rainfall extremes with short records – a comparison of MEV, Simplified MEV and point process methods. European Geosci. Union (EGU) General Assembly 2020 (Online). https://presentations.copernicus.org/EGU2020/EGU2020-6061_presentation.pdf.

Yin, S.Q., Wang, Z., Zhu, Z., Zou, X.K., Wang, W.T., 2018. Using Kriging with a heterogeneous measurement error to improve the accuracy of extreme precipitation return level estimation. J. Hydrol. 562, 518–529.

Zhang, Y., Long, M., Chen, K., Xing, L., Jin, R., Jordan, M.I., Wang, J., 2023. Skilful nowcasting of extreme precipitation with NowcastNet. Nature 619 (7970), 526–532.

Zorzetto, E., Botter, G., Marani, M., 2016. On the emergence of rainfall extremes from ordinary events. Geophys. Res. Lett. 43, 8076–8082. https://doi.org/10.1002/2016GL069445.

Zou, W.Y., Yin, S.Q., Wang, W.T., 2021. Spatial interpolation of the extreme hourly precipitation at different return levels in the Haihe River basin. J. Hydrol. 598, 126273.